Field-emission-induced growth of nanowire between electrodes

K. S. Yeong, J. B. K. Law, and J. T. L. Thong[a)]
Department of Electrical and Computer Engineering, Faculty of Engineering, National University of Singapore, 4 Engineering Drive 3, Singapore 117576, Singapore

(Received 24 January 2006; accepted 22 March 2006; published online 10 May 2006)

We demonstrate the growth of a tungsten nanowire between two microtip electrodes by the field-emission-induced growth process. A nanowire is grown from the cathode towards the opposing biased anode in a quasicontinuous manner. In order to study the nanowire growth process, the wire is grown in a stepwise manner until it bridges the cathode and the anode. The growth of the nanowire across the cathode-anode gap falls into four different regimes of initiation, steady growth, close-gap growth, and finally bridging of electrodes. The profile of the field-enhancement factor of the nanowire field emitter during growth matches the results from electrostatic modeling. © *2006 American Institute of Physics*. [DOI: 10.1063/1.2202733]

Field-emission-induced growth (FEIG) is a method to grow single conductive nanowires on sharp protrusions.[1,2] The ability to grow nanowires selectively by field emission from a sharp tip allows the technique to be applied to the fabrication of scanning probe microscope tips[3–5] and field emitters. In another application, Oon and Thong demonstrated the use of such nanowires as interconnects between two electrodes by overlaying the wire over an adjacent electrode, followed by fusing of the wire to the electrode.[6] This method requires a number of separate steps, including the initiation of nanowire growth, directing of the nanowire to the desired electrode, and finally wire fusing to the electrode to complete the connection. In this letter, we study the direct growth of a nanowire from the cathode to the anode until it bridges the two electrodes.

Typically, FEIG is carried out in a scanning electron microscope (SEM) specimen chamber, which allows *in situ* observation and characterization during and after nanowire growth. The FEIG growth of a tungsten nanowire is carried out in a stepwise manner in which the nanowire length is increased step by step towards the anode until the gap is bridged. The growth behavior and the voltage profile of the nanowire growing across the gap between the electrodes are discussed. As the nanowire grows, the local electric-field environment progressively changes. The evolving field-enhancement factor as the nanowire grows towards the anode is thus derived and compared with that obtained from electrostatic modeling.

The experiment is carried out in a Philips XL30 FEG ESEM (environmental scanning electron microscope). Two electrochemically etched tungsten tips are positioned by nanomanipulators such that they face each other, with a cathode-to-anode tip separation of 8 μm, as shown in Fig. 1(a). The growth process and mechanism are discussed in detail in Refs. 1 and 2.

In this study, a tungsten nanowire was grown in steps of several seconds starting from nanowire initiation, followed by a final continuous growth until it bridged the anode-to-cathode gap. During each growth period, field emission is used to grow the tungsten nanowire at a constant current of 100 nA, as regulated by the Keithley 237 source-measurement unit (SMU) that was used to bias the anode. With the tungsten carbonyl admitted, the chamber pressure was 3.5×10^{-5} mbar, from which the local vapor pressure in the vicinity of the nozzle was estimated to be about 10^{-2} mbar from the pumping speed and nozzle geometry. In between the growth periods, the precursor vapor source was closed. Before viewing by the SEM, we waited until the specimen chamber pressure decreased to a pressure in the range of 8×10^{-6} mbar to minimize tungsten and contamination growth by electron-beam-induced deposition. The nozzle was moved away and a closed-loop voltage sweep was then performed to determine the turn-on voltage (V_{on}) for 10 nA field emission current. An anode bias of around $V_{on}/2$ was applied to straighten the long and slender nanowire in order to take SEM micrographs for nanowire length measurement. All electrical measurements during growth or voltage sweeps were performed under computer control of the SMU.

A FEIG nanowire was grown in ten consecutive steps (6, 5, 5, 5, 11, 11, 10, 20, 10, and 10 s). Figure 1(a) shows the FEIG tungsten nanowire grown for the first nine periods just before it bridged the gap. The tungsten nanowire is on the tip of the cathode opposite to the anode indicated in the second micrograph. The cumulative growth time (T) and nanowire length (l) are indicated in each micrograph. Figure 1(b) shows the corresponding voltage profile to maintain a constant emission current of 100 nA during nanowire growth throughout all periods, each point representing 1 s of growth. A transmission electron microscopy (TEM) image of a FEIG tungsten wire grown for 2 s is shown in Fig. 2 and shows a polycrystalline/disordered tungsten core with a diameter of 5 nm and about 1 nm carbonaceous coating.

The FEIG nanowire growth from the cathode to the anode can be roughly divided into four stages, namely, initiation, steady growth, close-gap growth, and finally, bridging of electrodes. The growth starts with an initiation of the nanowire on the cathode tip which corresponds to the abrupt voltage drop from about 950 to ~100 V within 1 s, as shown in Fig. 1(b). The length of the nanowire at this juncture is about 200 nm while its diameter is around 5 nm, giving rise to a much higher field-enhancement factor β than the original cathode tip. As a result of the greatly enhanced local electric at the nanowire tip, a much lower voltage is now required for emission at the 100 nA growth current.

a)Author to whom correspondence should be addressed; electronic mail: elettl@nus.edu.sg

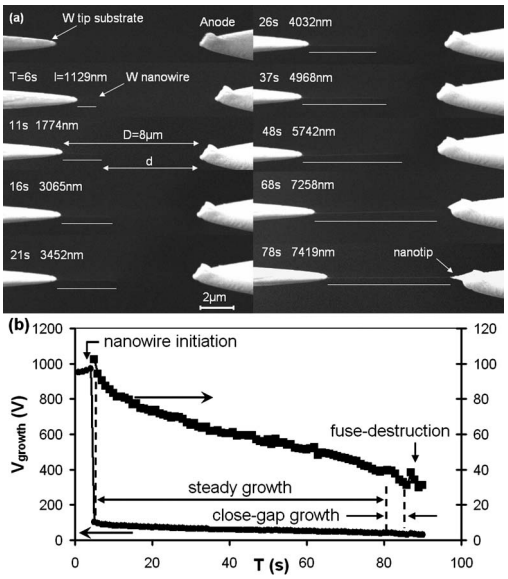

FIG. 1. (a) FEIG tungsten nanowire at different growth periods. Accumulated growth time (T) and nanowire length (l) are indicated in each micrograph. A line matching the length of each nanowire is drawn to provide a visual aid to indicate the length. Anode-cathode gap (D) is 8 μm. (b) Corresponding voltage profile at constant current (100 nA) during nanowire growth and detailed plot of the voltage profile after nanowire initiation.

The growth then enters a steady-growth regime, where the nanowire progressively lengthens towards the anode electrode. Here, the applied voltage reduces monotonically and gradually. The reduction in voltage is due to increasing β as the electrostatic geometry changes—the nanowire gets longer while the cathode-to-anode gap reduces.

The growth process then enters the close-gap regime in the 69–78 s period. In addition to the nanowire growth, a nanotip was observed to form on the anode tip in this growth period. Material growth on the anode is mainly due to electron-beam-induced deposition (EBID) since the density of electrons that impinge directly on the apex of the anode increases as the gap reduces. These electrons, accelerated to about 40 eV kinetic energy, will crack $W(CO)_6$ molecules adsorbed on the anode surface and results in the deposition of carbon-rich tungsten material on the anode surface.[7,8] The presence of a strong electric field at the anode may also contribute to the anode deposition as well. In scanning-tunneling microscope deposition from $Fe(CO)_5$, Kent *et al.* showed that carbon-rich nanostructures were found on both the STM tip and the negatively biased substrate.[8] They believed that a high local electric field is necessary to form such structures.

The final stage of growth (79–88 s) involved bridging of the nanowire and the nanotip which triggered the destruction of the nanowire, corresponding to the instant just before the sudden voltage increase shown in Fig. 1(b). When the nanowire and the nanotip first contacted, the ~30 V potential difference between the two induced a current spike which destroyed the weak joint immediately. As a result, the nanowire fused, and its length was reduced to about 7 μm after the catastrophic event, evidenced by the voltage jump. Following this, the voltage after the jump decreased gradually as the shortened nanowire regrew after a 100 nA emission current was restored by the voltage supply. The growth continued until it bridged the gap once more and triggered another cycle of fuse destruction and regrowth. A successful interconnect can be achieved by insertion of series resistance and by minimizing stray capacitances in the circuit to reduce the current spike.

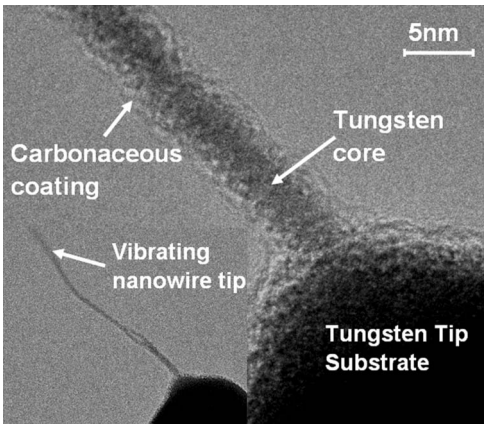

FIG. 2. TEM images of FEIG nanowire taken by a JEOL 2010F TEM at 200 kV.

The nature of the change in voltage required to maintain constant-current growth is due to the change in β as the nanowire lengthened. The β profile can be derived from the turn-on voltage (V_{on} for 10 nA) from a closed-loop voltage sweep as shown below. V_{on} as a function of nanowire length is shown in Fig. 3. The turn-on voltage before nanowire initiation is about 900 V (not shown) and drops to less than 80 V after initiation. Only V_{on} for the first eight growth periods is plotted and used for the derivation of β. Since the anode geometry changes progressively and significantly in the last two growth periods, the electric field has not been modeled, but such geometrical changes will inevitably complicate the analysis of changes in β.

Field emission is described by the Fowler-Nordheim equation, where the field emission current I is [9]

$$I = A\frac{e^3E^2}{8\pi h\phi t^2(y)}\exp\left[-\frac{8\pi\sqrt{2m}\phi^{3/2}}{3heE}\nu(y)\right], \tag{1}$$

$$y = \frac{\sqrt{e^3E}}{\phi}. \tag{2}$$

To a good approximation, $t^2(y)=1.1$ and $\nu(y)=0.95-y^2$, and the equation simplifies to

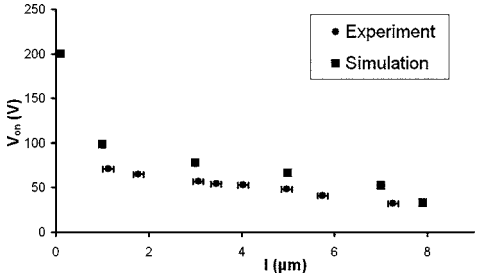

FIG. 3. Turn-on voltage V_{on} for 10 nA emission current obtained from a closed-loop voltage sweep for the first eight growth periods as a function of nanowire length. Error in the estimation of nanowire length from SEM micrograph is indicated. V_{on} obtained from simulation is shown for comparison.

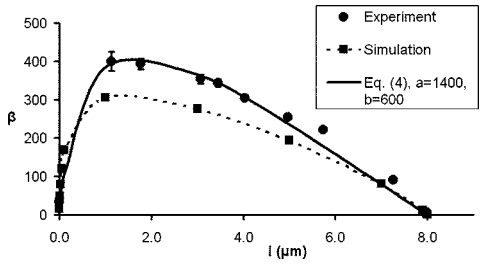

FIG. 4. Experimental and simulated β profiles during nanowire growth. *Y*-error bars indicate error in estimating nanowire length from SEM micrograph. β from Eq. (4) is shown for comparison.

$$I = A\frac{1.5\times10^{-6}E^2}{\phi}\exp\left(\frac{10.4}{\sqrt{\phi}}\right)\exp\left(\frac{-6.44\times10^{9}\phi^{3/2}}{E}\right), \tag{3}$$

where ϕ is the work function, A is the emission area, r is the nanowire tip radius, and E is the electric field in V/m. Substituting $I=10$ nA, $A=\pi r^2$, where $r=2.5$ nm, and a work function of 4.50 eV for a clean tungsten microtip[10,11] into Eq. (3) gives a turn-on electric field of $E_{on}=4.42\times10^9$ V/m at the nanowire tip. Since the nanowire diameter and the work function are constant, and the anode geometry does not change throughout the first eight periods after initiation, the electric field at the nanowire tip at turn on should remain at 4.42×10^9 V/m, irrespective of the nanowire length. β changes are solely due to changes in the nanowire length. Thus, β, defined as the ratio of the local electric field at the tip E_{tip} to the global electric field E_{global}, is given by[12,13]

$$\beta = \frac{E_{tip}}{E_{global}} = \frac{E_{on}}{V_{on}/(D-l)}, \tag{4}$$

which is plotted in Fig. 4. In order to confirm the results, we compared the results with simulation data. The simulation was carried out using the Charged Particle Optics 2DS program with a well-defined cathode, anode, and nanowire geometry that resembles the actual configuration. The simulated nanowire length spans from 5 to 7995 nm. The derived β and V_{on} are shown in Figs. 4 and 3 for comparison with the experimental data.

Both the experimental and simulated β exhibit similar trends as the nanowire grows across the gap. The discrepancy in the value of β could be due to the use of the crystalline tungsten work function of 4.50 eV for the nanowire tip, which is both partially disordered and likely to be covered with adsorbates. A replot with a nanowire tip work function of 3.82 eV eliminates the discrepancy between the experimental and simulation β profile; the lower work function value is quite reasonable considering the tip roughness and adsorbed species at the growing tip. β increases rapidly right after nanowire initiation until it peaks at about 1.5 μm. The initial rapid increase is due to a significant reduction of emission tip size after initiation and the reduction in field screening from the underlying microtip as the nanowire grows away from it. β then decreases gradually in the steady-growth regime due to rapid increase of E_{global} as the cathode-anode gap decreases. In the very-close-gap regime, β will approach unity as the nanowire tip and anode approach a parallel-plate configuration. The β profile can be described by Eq. (5),

$$\beta = \left(\frac{l}{r}+2\right)\left(1-\frac{l}{D}\right)f(l), \tag{5}$$

$$f(l) = \frac{a}{l+b}, \tag{6}$$

where l is the nanowire length, and a and b are arbitrary constants chosen to obtain the best fit with the experimental data. Equation (5) with the function $f(l)$ omitted describes β of a rod with a hemispherical cap extending perpendicular from a cathode plate towards a parallel anode plate separated by a fixed gap.[14,15] The function $f(l)$ is added to take into account the contribution of the cathode base tip to the overall β of the nanowire.[16]

In conclusion, we studied the FEIG growth of a nanowire step by step until it bridged the gap between the cathode and the anode. The growth can be demarcated into an initiation stage, followed by a steady-growth stage, a close-gap regime, and finally bridging of the two electrodes. The evolution of the field-enhancement factor β as the nanowire grows across the gap between electrodes is also derived. The β profile shows a good match with simulation results.

[1] J. T. L. Thong, C. H. Oon, M. Yeadon, and W. D. Zhang, Appl. Phys. Lett. **81**, 4823 (2002).
[2] C. H. Oon, S. H. Khong, C. B. Boothroyd, and J. T. L. Thong, J. Appl. Phys. **99**, 064309 (2006).
[3] C. H. Oon, J. T. L. Thong, Y. Lei, and W. K. Chim, Appl. Phys. Lett. **81**, 3037 (2002).
[4] A. B. H. Tay and J. T. L. Thong, Appl. Phys. Lett. **84**, 5207 (2004).
[5] A. B. H. Tay and J. T. L. Thong, Rev. Sci. Instrum. **75**, 3248 (2004).
[6] C. H. Oon and J. T. L. Thong, Nanotechnology **15**, 687 (2004).
[7] D. B. Bidinosti and N. S. McLntyre, Can. J. Chem. **4**, 641 (1961).
[8] A. D. Kent, T. M. Shaw, S. V. Molnar, and D. D. Awschalom, Science **262**, 1249 (1993).
[9] I. Brodie and C. A. Spindt, in *Advances in Electronics and Electron Physics*, edited by P. W. Hawkes, B. Kazan, and T. Mulvey (Academic, San Diego, CA, 1992), Vol. 83, Chap. 1, pp. 2–95.
[10] W. P. Dyke and W. W. Dolan, in *Advances in Electronics and Electron Physics*, edited by L. Marton (Academic, New York, 1956), Vol. 8, Chap. III, pp. 90–182.
[11] F. Ashworth, in *Advances in Electronics*, edited by L. Marton (Academic, New York, 1951), Vol. 13, Chap. 1, pp. 1–41.
[12] R. C. Smith, R. D. Forrest, J. D. Carey, W. K. Hsu, and S. R. P. Silva, Appl. Phys. Lett. **87**, 013111 (2005).
[13] R. C. Smith, D. C. Cox, and S. R. P. Siva, Appl. Phys. Lett. **87**, 103112 (2005).
[14] H. C. Miller, J. Appl. Phys. **38**, 4501 (1967).
[15] R. G. Forbes, C. J. Edgcombe, and U. Valdre, Ultramicroscopy **95**, 7 (2003).
[16] J. Y. Huang, K. Kempa, S. H. Jo, S. Chen, and Z. F. Ren, Appl. Phys. Lett. **87**, 053110 (2005).